

# Cold hybrid electrical-optical ion trap

Jin-Ming Cui,<sup>1,2,3,\*</sup> Shi-Jia Sun,<sup>1,2</sup> Xi-Wang Luo,<sup>1,2,†</sup> Yun-Feng Huang,<sup>1,2,3</sup> Chuan-Feng Li,<sup>1,2,3,‡</sup> and Guang-Can Guo<sup>1,2</sup>

<sup>1</sup>CAS Key Laboratory of Quantum Information, University of Science and Technology of China, Hefei 230026, China

<sup>2</sup>CAS Center for Excellence in Quantum Information and Quantum Physics, University of Science and Technology of China, Hefei 230026, China

<sup>3</sup>Hefei National Laboratory, University of Science and Technology of China, Hefei 230088, China

(Dated: June 21, 2023)

Advances in research such as quantum information and quantum chemistry require subtle methods for trapping particles (including ions, neutral atoms, molecules, etc.). Here we propose a hybrid ion trapping method by combining a Paul trap with optical tweezers. The trap combines the advances of the deep-potential feature for the Paul trap and the micromotion-free feature for the optical dipole trap. By modulating the optical-dipole trap synchronously with the radio frequency voltage of the Paul trap, the alternating electrical force in the trap center is fully counteracted, and the micromotion temperature of a cold trapped ion can reach the order of nK while the trap depth is beyond 300K. These features will enable cold collisions between an ion and an atom in the  $s$ -wave regime and stably trap the produced molecular ion in the cold hybrid system. This will provide a unique platform for probing the interactions between the ions and the surrounding neutral particles and enable the investigation of new reaction pathways and reaction products in the cold regime.

*Introduction.*— Cold chemistry near absolute zero reveals quantum process in the reaction process, which attracts interests in both chemical and physical fields [1–12]. In the last decade, an emerging area of cold hybrid ion-atom systems has been developed as a new platform for fundamental research, which is dedicated to controlling the cold collision and quantum chemistry of ions and atoms [13–19]. Besides, binding the neutral atom and ion and then stably trapping the produced molecular ion are prerequisites for exploring the quantum features of the molecular ion. To investigate collision physics in the quantum regime of the cold hybrid ion-atom system, reaching the single partial wave limit (i.e., the  $s$ -wave limit) is an important step [14]. Although the trapped ion can be cooled close to the quantum collision regime using buffer atomic gases with a large ion-atom mass ratio [20], the micromotion of the Paul trap (PT) heats the system away from a stable bound state [21–23], which hinders progress in this area. Pioneering experiments using optical dipole traps (ODTs) to capture ions were demonstrated [24–27], which is a potential solution to the micromotion heating problem in the cold hybrid ion-atom system. However, because the dipole potential is shallow, it is quite challenging to keep the ion during the reaction and stably trap the produced molecular ion.

In this work, we propose a novel hybrid electrical-optical ion trap that combines the advantages of the deep-potential feature of a PT and the micromotion-free feature of an ODT. The key idea is to counteract the alternating electrical force around the center of a PT that is responsible for the micromotion problem, which is achieved by introducing optical-dipole traps that are modulated synchronously with the radio frequency (RF) voltage of the PT. This hybrid electrical-optical trap corresponds to a deep PT with a micromotion-free dip at

the center, and this potential structure provides an ideal platform for studying low-energy physics (such as cold collisions and cold chemistry). Since the center dip provides a micromotion-free area for the trapped ion to interact with a neutral atom, the produced molecular ion can be stably kept in a deep background potential profile provided by the PT. To analyze the performance of the trap, we consider counteracting 99% of the alternating force which is experimentally reasonable. The intrinsic micromotion (iMM) energy can be suppressed by four orders of magnitude. Under current voltage compensation techniques in trapped ion fields [28], the DC stray field can be suppressed below 1 V/m, which leads to the ultimate cold ion excess micromotion (eMM) temperature in the hybrid trap below 1 nK. Under such cold ion temperatures, many ion-atom  $s$ -wave scattering process can be investigated. Moreover, by simulating a cold collision process between a  $\text{Yb}^+$  ion and a Rb atom, we find that the hybrid trap effectively solves the micromotion heating problem, which dissociates the ion-atom bound state in the cold collision process. The proposed hybrid trap offers a simple yet powerful platform to study ion-atom collisions in the quantum regime, which paves the way for exploring novel reactions and manipulating the produced molecular ion in such cold hybrid systems.

*Scheme and Results.*— Our scheme employs modulating optical tweezers to counteract the alternating force caused by the RF electrical field. If we consider a hybrid trap consisting of a PT and  $N$  modulating ODTs, the total potential of the trap is

$$U(\mathbf{r}, t) = U_E(\mathbf{r}) + \tilde{U}_E(\mathbf{r}) \cos(\Omega t) + \sum_i^N U_{D,i}(\mathbf{r}) [1 + \eta_i \cos(\Omega t)], \quad (1)$$

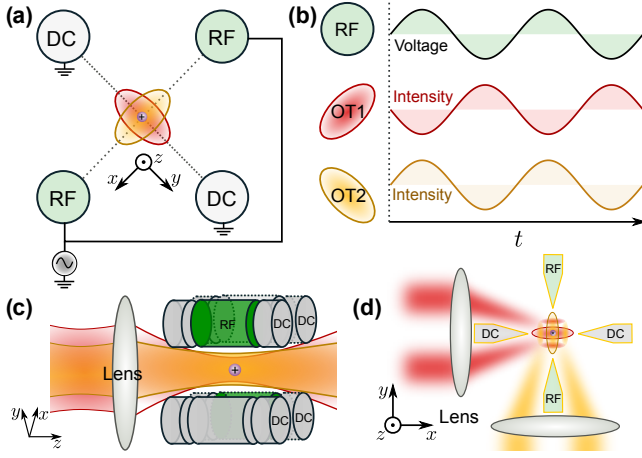


FIG. 1. Scheme of a hybrid electrical-optical ion trap. (a) The trap consists of a Paul trap (e.g., a four-rod trap or a blade trap) and two modulating optical dipole traps (ODTs) with different oriented astigmatic spots. (b) The phase relation between the RF voltage of the Paul trap and the optical intensities of the two ODTs. (c, d) two feasible realizations of the hybrid trap.

where  $U_E(\mathbf{r})$  and  $\tilde{U}_E(\mathbf{r})$  are the potentials generated by the DC field and RF field of the PT respectively,  $U_{D,i}(\mathbf{r})$  is the potential of  $i$ 'th ODT, and  $\eta_i$  is the modulation depth of  $i$ 'th ODT with  $|\eta_i| \leq 1$ . Supposing the centers of all traps overlap each other for simplicity, the potentials around the trap center can be expanded as harmonic forms as

$$\begin{aligned} U_E(\mathbf{r}) &= k_0^x x^2 + k_0^y y^2 + k_0^z z^2 + C_E, \\ \tilde{U}_E(\mathbf{r}) &= k_1^x x^2 + k_1^y y^2 + k_1^z z^2 + \tilde{C}_E, \\ U_{D,i}(\mathbf{r}) &= K_i^x x^2 + K_i^y y^2 + K_i^z z^2 + C_{D,i}, \end{aligned}$$

where  $C_E$ ,  $\tilde{C}_E$  and  $C_{D,i}$  are constants.  $U_E(\mathbf{r})$  and  $\tilde{U}_E(\mathbf{r})$  generated by electrical fields have to fulfill the Laplace equation  $\Delta U(\mathbf{r}) = 0$ , which leads to restrictions in the geometric factors,

$$k_0^x + k_0^y + k_0^z = 0, \quad (2)$$

$$k_1^x + k_1^y + k_1^z = 0, \quad (3)$$

while  $U_{D,i}(\mathbf{r})$  is not restricted by this condition. The alternating force strength of the hybrid trap is  $\tilde{\mathbf{F}}(\mathbf{r}) = \nabla(\tilde{U}_E + \sum \eta_i U_{D,i})$ , so eliminating the force to zero leads to the condition

$$k_1^\gamma + \sum_i \eta_i K_i^\gamma = 0, \quad (4)$$

for all  $\gamma \in \{x, y, z\}$ , which can be achieved by setting the modulation depths and geometric shapes of ODTs.

Supposing we use astigmatic Gaussian spots to generate the dipole traps required. The intensity profile of a

focused astigmatic Gaussian beam along axis  $c$  in coordinate  $(\hat{a}, \hat{b}, \hat{c})$  can be written as

$$I(\mathbf{r}) = I_0 \frac{w_{0a}}{w_a(c)} \frac{w_{0b}}{w_b(c)} \exp \left\{ -2 \left[ \frac{a^2}{w_a(c)^2} + \frac{b^2}{w_b(c)^2} \right] \right\}, \quad (5)$$

where  $w_{a/b}(c) = w_{0,a/b} \sqrt{1 + (c/z_{Ra/b})^2}$  are the beam waists for  $a$  and  $b$  axes, i.e., short and long axes respectively,  $z_{Ra/b} = \pi w_{0,a/b}^2 / \lambda$  are the Rayleigh ranges and  $\lambda$  is the wavelength. As the potential of ODT is proportional its intensity  $U_{D,i}(\mathbf{r}) \propto I_{D,i}(\mathbf{r})$ , by expanding it near the zero point, the potential coefficients are

$$\begin{aligned} K_i^a &= \frac{2U_{0i}}{w_{0,ai}^2}, K_i^b = \frac{2U_{0i}}{w_{0,bi}^2}, \\ K_i^c &= \frac{U_{0i} \lambda^2}{2\pi^2} \left( \frac{1}{w_{0,ai}^4} + \frac{1}{w_{0,bi}^4} \right), \end{aligned} \quad (6)$$

where  $U_{0i} = \frac{\pi c^2 \Gamma}{2\omega_0^3} \left( \frac{2}{\Delta_2} + \frac{1}{\Delta_1} \right) I_{0i}$  [29]. Finding a proper set of  $\{\eta_i U_{0i}, w_{0,ai}, w_{0,bi}\}$  to satisfy Eq. 4 and Eq. 6 will eliminate the alternation force at the trap center.

Figure 1(c,d) shows two feasible configurations to demonstrate the scheme in a symmetric linear PT with four rods or blades [30, 31]. For simplicity, we take Fig. 1(c) for example, where two optical tweezers with focused astigmatic Gaussian spots are applied on the trapped ion with similar beam waists, i. e.,  $w_{0,a1} = w_{0,a2} = w_a$ ,  $w_{0,b1} = w_{0,b2} = w_b$ ,  $U_{01} = U_{02} = U_0$ , and the two trap long axes are perpendicular to each other, i.e.  $\hat{a}_1 \perp \hat{a}_2 \parallel \hat{y}$ ,  $\hat{b}_1 \perp \hat{b}_2 \parallel \hat{x}$ . The symmetric linear PT condition requires  $k_1^x = -k_1^y = k_1$ ,  $k_1^z = 0$ . Suppose  $\eta_1 = -\eta_2 = 1$ , which indicates modulations between two ODTs have a  $\pi$  phase difference (shown in Fig. 1(b)), then the configurations of the ODTs can be

$$\begin{aligned} k_1 &= k_a - k_b, \\ K_1^x &= K_2^y = k_a, \\ K_1^y &= K_2^x = k_b, \end{aligned} \quad (7)$$

where  $k_{a,b} = 2U_0/w_{a,b}^2$ .

The pseudo potential of the hybrid trap can be decomposed into a direct potential (DP) and an alternating potential (AP)

$$\Psi(\mathbf{r}) = \Phi_0(\mathbf{r}) + \frac{1}{4m\Omega^2} \|\nabla\Phi_1(\mathbf{r})\|^2, \quad (8)$$

where  $\Phi_0(\mathbf{r}) = U_E(\mathbf{r}) + \sum_i U_{D,i}(\mathbf{r})$  and  $\Phi_1(\mathbf{r}) = \tilde{U}_E(\mathbf{r}) + \sum_i \eta_i U_{D,i}(\mathbf{r})$  are the direct and alternating potentials respectively. For a symmetric linear PT [30],  $k_0^x = k_0^y = -2k_0^z = -2\kappa QV_{DC}/Z_0^2$ ,  $k_1^x = -k_1^y = QV_{RF}/2R^2$ ,  $k_1^z = 0$ , where  $\kappa$  is a geometric factor of the trap,  $Q$  is the charge of the ion,  $V_{DC}$  and  $V_{RF}$  are the DC and RF voltages applied to the trap,  $R$  is the perpendicular distance from the trap axis to the trap electrodes,  $Z_0$  is the distance from the trap center to the endcap

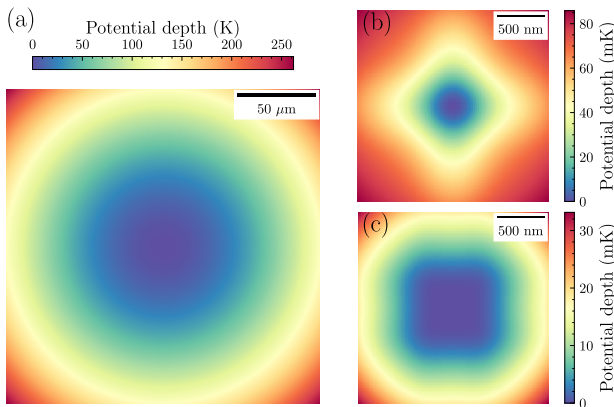


FIG. 2. Pseudo potential of a hybrid trap for  $^{171}\text{Yb}^+$ . (a) The total pseudo potential of the trap, indicating a deep potential. (b,c) The constant part and the alternating part of the pseudo potential near the trap center, respectively. The alternating pseudo potential is flat near the center, which indicates the alternating force is zero. The simulation condition is  $\Omega = 2\pi \times 2$  MHz,  $V_{RF} = 10$  V,  $\kappa = 0.6$ ,  $V_{DC} = 1$  V,  $R = 0.5$  mm,  $Z_0 = 1$  mm,  $\omega_x = \omega_y = 2\pi \times 180$  kHz,  $\omega_z = 2\pi \times 131$  kHz for the Paul trap, laser wavelength at 554.6 nm,  $w_a = w_b/3 = 478$  nm can be generated through an objective with a numerical aperture (NA) of 0.6,  $U_0/h = -622$  MHz for optical dipole traps.

electrodes. The pseudo potential can be calculated by substituting Eq. 5-7 into Eq. 8. When the alternating force caused by the RF electrical field is completely compensated by the modulating ODTs, which we call the zero alternating trapping condition (ZATC), we can derive  $U_0 = QV_{RF}w_a^2w_b^2/4R^2(w_a^2 - w_b^2)$ . To make the condition realistic, a low RF voltage of PT and small spots of ODTs should be used to minimize the optical power of the ODT. Consequently, a lower RF frequency  $\Omega$  is preferred to make a deeper pseudo potential under the low RF voltage. A numerical simulation result is shown in Fig. 2. In a large range, it acts as a PT with deep potential as Fig. 2(a). At the center of the trap, it acts as a tight ODT as Fig. 2(b). The alternating pseudo potential in Fig. 2(c) is flat, which indicates the alternating force is zero. With the simulation result, the required laser power is 0.7 W at 554.6 nm, if we use an objective with NA=0.6 to generate the required ODTs.

Next, we will discuss the cold trapped ion temperature limit in the hybrid trap. Supposing the ion oscillates near  $\mathbf{u}_0$  in the hybrid trap under a stray electrical field  $\mathbf{E}$ , and has been cooled to a low temperature  $|\mathbf{u} - \mathbf{u}_0| \ll w_a$ , then the motion equation can be approximated as a Mathieu equation near  $\mathbf{u}_0$

$$\ddot{u}_l + [a_l(\mathbf{u}_0) + 2q_l(\mathbf{u}_0) \cos(\Omega t)] \frac{\Omega^2}{4} u_l = \frac{Q \cdot E_l}{m}, \quad (9)$$

where  $a_l(\mathbf{u}) = 4\hat{\epsilon}_l \cdot \nabla \Phi_0(\mathbf{u})/m\Omega^2 u_l$  and  $q_l(\mathbf{u}) = 2\hat{\epsilon}_l \cdot \nabla \Phi_1(\mathbf{u})/m\Omega^2 u_l$ . The equilibrium position  $\mathbf{u}_0$  can be nu-

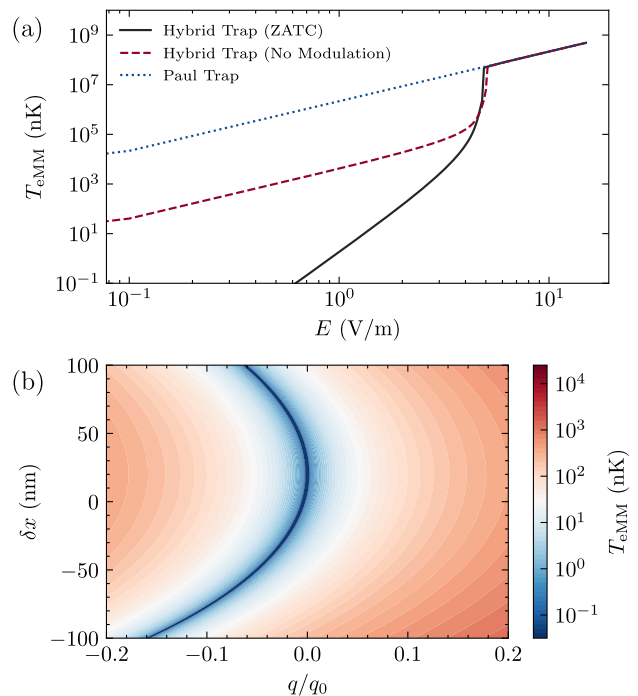


FIG. 3. Ion motion simulation for trapping temperature in a stray electrical field (SEF). (a) Excess micromotion (eMM) temperature of a trapped ion along with different SEFs. The hybrid trap provides a lower temperature than a PT under the same SEF. When the hybrid trap works at zero alternating trapping condition (ZATC), the ion's eMM temperature reaches nK under a SEF of 1 V/m. The direction of the SEF for simulation is (1,1,1). (b) Ion's eMM temperature simulation under experimental imperfections,  $\delta x$ : misalignment between Paul trap and the ODT,  $\Delta q$ : uncompensated alternating force factor. The figure is calculated under a SEF of 1 V/m along the  $x$  axis. Hybrid trap and Paul trap parameters are the same as those in Fig. 2.

merically solved by iterating

$$u_{0,l} = \frac{4Q \cdot E_l}{m\Omega^2 [a_l(\mathbf{u}) + q_l^2(\mathbf{u})/2]}. \quad (10)$$

The final temperature caused by excess micromotion is

$$T_{\text{eMM}} = \frac{m\Omega^2}{16k_B} \sum_l q_l^2(\mathbf{u}_0) u_{0,l}^2. \quad (11)$$

Using the above numerical method, we can study the ion eMM temperature under a large electrical field. Fig. 3(a) shows the comparison of trapped ion eMM temperature in three different traps under a stray electrical field along the (1,1,1) direction. The stray field will shift the trap center of the PT part of the hybrid trap while the ODT is not affected, so the total pseudo potential is a double well under a small stray field. The ion stays in the tight ODT under a small stray field, and the ion's eMM temperature will be low even without modulating the ODTs. By increasing the stray field, the ion will eventually be

TABLE I. ODT laser wavelengths of hybrid ion traps for different ion-atom systems.

Ion	Atom	$\lambda_{\text{ODT}}$ (nm)	$P$ (W)	$E_k/k_B$ (nK)
Yb <sup>+</sup>	Rb	420.6	0.24	44.7
Yb <sup>+</sup>	Rb	422.3	0.25	44.7
Yb <sup>+</sup>	Rb	787.4	1.48	44.7
Yb <sup>+</sup>	Yb	554.63	0.70	44.7
Ca <sup>+</sup>	Na	589.46	0.48	1370.7
Ca <sup>+</sup>	Li	670.97	1.09	10601.5
Sr <sup>+</sup>	Rb	787.41	0.94	77.8

pushed from the ODT to PT, so the ion's eMM temperature of the hybrid trap is close to that of the PT, when the stray field is larger than 5 V/m.

In order to further insight the ion eMM temperature relation with experiment parameters (e. g., misalignment between PT and the ODT  $\delta x$ , stray electrical field  $E$ , residual alternating force (RAF) parameter  $\Delta q = 4(k_1 + k_a - k_b)/m\Omega^2$ ), we study one dimensional motion for simplification. Considering the condition of small misaligned distance  $\delta x \ll w_0$ , the approximated ion eMM temperature can be derived as [32]

$$T_{\text{eMM}} \approx \frac{m\Omega^2}{16k_B} \left( \Delta q + \frac{(\delta x - x_0)^2}{x_b^2} \right)^2 x_0^2, \quad (12)$$

where  $x_0 \approx -Q \cdot E / (k_0 + 2k_a + 2k_b)$  is the ion position offset pushed by the stray electrical field, and  $x_b^2 = m\Omega^2 / 8(k_b/w_b^2 - k_a/w_a^2)$ . Fig. 3(b) shows that the ion eMM temperature can reach 100 nK level even with a misalignment about 50 nm and 5% of RAF, under 1 V/m stray field along the  $x$  axis. Several ion imaging methods with a position accuracy below 10 nm have been demonstrated [33–35], which can be used to compensate the misalignment in future. The ion iMM temperature and energy is proportional to  $\Delta q^2$  [32], which can also be significantly reduced by four orders of magnitude with 1% RAF.

Finally, we will investigate the collision process between an ion and an atom in the hybrid trap. To perform this study, we note that the laser wavelength of the ODT should be specified for a given composition of ion and atom elements. The alternating ODT should not affect the ground state of the atom, otherwise, the alternating ODT will drive atom motion when the atom approaching the ion. Tab. I lists several laser wavelengths for some composition of ion-atom species, and the laser power with hybrid trap setting as Fig. 2. We take Rb and Yb<sup>+</sup> in this investigation following the method presented in Ref. [21], with details in [32]. When an ion moves in a PT without any disturbance, the RF field does zero work on the ion for an RF period. However, in the cold hybrid ion-atom system, the polarized atom will exert an attraction force on the ion (by attraction potential  $V(r) = -C_4/r^4$ ) and

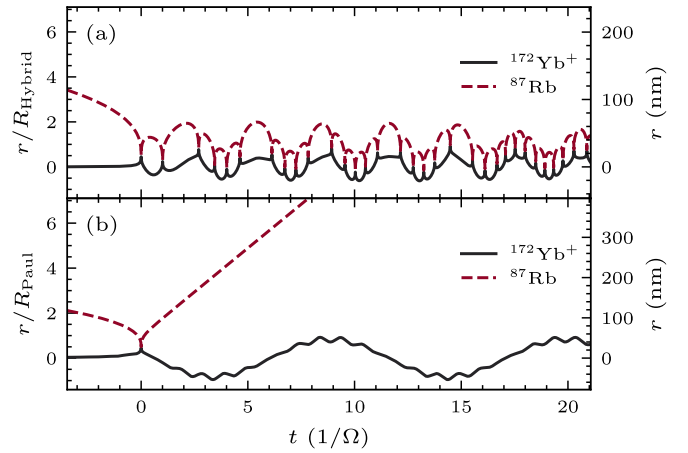


FIG. 4. Numerical simulations of a ion-atom (Rb and Yb<sup>+</sup>) collision in a hybrid trap (a) and a Paul trap (b). For comparison, the hybrid trap has the same electric fields with configurations as Fig. 2. Rb approaching an Yb<sup>+</sup> initially stationed in trap center, the first hard-core collision time is at  $t = 0$ . In Paul trap, the ion is heated by the RF field and bounces out quickly, whereas in hybrid trap, the ion-atom can be weakly bounded. The harmonic frequencies of two traps are  $\omega_{\text{Hybrid}} = 2\pi \times 0.84$  MHz and  $\omega_{\text{Paul}} = 2\pi \times 0.18$  MHz, leading to the corresponding characteristic lengths  $R_{\text{Hybrid}} = 33.4$  nm and  $R_{\text{Paul}} = 55.9$  nm, respectively. The simulation method is modified from Ref. 21.

thus disturb the conserved cycle of energy transfer, and finally the ion-atom system gains net energy from the RF field, which increases the temperature of the system. A characteristic length scale  $R = \sqrt[6]{2C_4/m_i\omega^2}$  is preferred to be used (when the interaction potential  $V(r)$  is equal in magnitude to the trap harmonic potential, where  $\omega = \Omega\sqrt{a + q^2/2}/2$  is the secular frequency of the ion near the trap center). In a PT (Fig. 4(b)), the ion gains enough energy from the RF field when the atom approaches, and after one collision, the atom escapes. In the hybrid trap (Fig. 4(a)), since the alternating force induced by the RF field near the trap center is compensated, the ion-atom system nearly undergoes an energy-conservative process and forms a weakly bound ion-atom pair, keeping a low temperature. In the hybrid trap, the corresponding characteristic energy scale is no longer restricted by the RF heating but determined by the atomic gas temperature, which enables access to the regimes of the  $s$ -wave limit or quantized ion motion in the cold hybrid system. The work done by the RAF during a collision depends on the phase  $\phi$  at the time of the close-range collision, which can be written as [32]

$$W = \frac{1}{2}\mu\Omega^2 R^2 \sin \phi \cdot \left( \Delta q \eta_1 + \frac{R^4}{r_0^2 x_b^2} \eta_2 \right)$$

where  $\mu = m_i m_a / (m_i + m_a)$  is the reduced mass,  $\eta_1 = 2/3 \int_0^{\Omega t_1} (A - B\tau^{1/3}) \cdot \tau^{-2/3} \sin \tau \cdot d\tau$  and  $\eta_2 = 2/3 \int_0^{\Omega t_1} (A - B\tau^{1/3})^3 \cdot \tau^{-2/3} \sin \tau \cdot d\tau$  are integrates with

parameters  $A = r_c r_0 / R^2$ ,  $B = \mu r_0^2 / m_i R^2$ , the ion's displacement from the trap center  $r_c$  for the collision position and a characteristic length  $r_0 = \sqrt[6]{18C / \mu \Omega^2}$ . Fig. 4(a) shows  $r_c$  is distributed in  $0 \sim 20$  nm for multi hard-core collisions, indicating that the max work done by RAF for one collision is on the order of tens of nK $\cdot k_B$ .

*Conclusion and discussion.*— In summary, we proposed a novel hybrid trap consisting of a PT and modulated ODTs that takes advantage of the deep-potential feature of the PT while eliminating the micromotion problem in the cold hybrid ion-atom system. The trap can suppress the micromotion temperature to the order of nK, offering a new route to reach the quantum collision in the ion-atom mixture. Our proposed schemes are quite feasible since an ion trap system with high optical accessibility has been demonstrated in [36]. Compared with previous optical trapping methods for ions where the PT is switched off [24–27], our scheme can stably trap elementary and molecular ions all through the cold ion-atom collision process due to the always-on PT, which provides an ideal platform for studying cold ion-atom collision and reaction and investigating the properties of the produced molecular ion.

This work was supported by the National Natural Science Foundation of China (Grants No. 11774335, No. 11734015, and No. 12204455), the Key Research Program of Frontier Sciences, CAS (Grant No. QYZDY-SSW-SLH003), the Science Foundation of the CAS (Grant No. ZDRW-XH-2019-1), the Fundamental Research Funds for the Central Universities (Grants No. WK2470000027, and No. WK2470000028), Innovation Program for Quantum Science and Technology (Grants No. 2021ZD0301604, and No. 2021ZD0301200).

J.-M. Cui and S.-J. Sun contributed equally to this work.

---

\* jmcui@ustc.edu.cn

† luoxw@ustc.edu.cn

‡ cfi@ustc.edu.cn

- [1] B. R. Heazlewood and T. P. Softley, *Nature Reviews Chemistry* **5**, 125 (2021).
- [2] X. He, K. Wang, J. Zhuang, P. Xu, X. Gao, R. Guo, C. Sheng, M. Liu, J. Wang, J. Li, G. V. Shlyapnikov, and M. Zhan, *Science* **370**, 331 (2020).
- [3] M.-G. Hu, Y. Liu, D. D. Grimes, Y.-W. Lin, A. H. Gheorghie, R. Vexiau, N. Bouloufa-Maafa, O. Dulieu, T. Rosenband, and K.-K. Ni, *Science* **366**, 1111 (2019).
- [4] J. T. Zhang, Y. Yu, W. B. Cairncross, K. Wang, L. R. B. Picard, J. D. Hood, Y.-W. Lin, J. M. Hutson, and K.-K. Ni, *Physical Review Letters* **124** (2020), 10.1103/physrevlett.124.253401.
- [5] J. D. Hood, Y. Yu, Y. W. Lin, J. T. Zhang, K. Wang, L. R. Liu, B. Gao, and K. K. Ni, *Physical Review Research* **2** (2020), 10.1103/physrevresearch.2.023108.
- [6] Y. Liu and K.-K. Ni, *Annual Review of Physical Chemistry* **73**, 73 (2022).
- [7] H. Yang, X.-Y. Wang, Z. Su, J. Cao, D.-C. Zhang, J. Rui, B. Zhao, C.-L. Bai, and J.-W. Pan, *Nature* **602**, 229 (2022).
- [8] Z. Su, H. Yang, J. Cao, X.-Y. Wang, J. Rui, B. Zhao, and J.-W. Pan, *Physical Review Letters* **129** (2022), 10.1103/physrevlett.129.033401.
- [9] J. Cao, H. Yang, Z. Su, X.-Y. Wang, J. Rui, B. Zhao, and J.-W. Pan, *Physical Review A* **107** (2023), 10.1103/physreva.107.013307.
- [10] L. W. Cheuk, L. Anderegg, Y. Bao, S. Burchesky, S. S. Yu, W. Ketterle, K.-K. Ni, and J. M. Doyle, *Physical Review Letters* **125** (2020), 10.1103/physrevlett.125.043401.
- [11] Y. Xie, H. Zhao, Y. Wang, Y. Huang, T. Wang, X. Xu, C. Xiao, Z. Sun, D. H. Zhang, and X. Yang, *Science* **368**, 767 (2020).
- [12] T. de Jongh, M. Besemer, Q. Shuai, T. Karman, A. van der Avoird, G. C. Groenenboom, and S. Y. T. van de Meerakker, *Science* **368**, 626 (2020).
- [13] A. Härter and J. H. Denschlag, *Contemporary Physics* **55**, 33 (2014).
- [14] M. Tomza, K. Jachymski, R. Gerritsma, A. Negretti, T. Calarco, Z. Idziaszek, and P. S. Julienne, *Reviews of Modern Physics* **91**, 035001 (2019).
- [15] N. Zuber, V. S. V. Anasuri, M. Berngruber, Y.-Q. Zou, F. Meinert, R. Löw, and T. Pfau, *Nature* **605**, 453 (2022).
- [16] Y.-Q. Zou, M. Berngruber, V. S. V. Anasuri, N. Zuber, F. Meinert, R. Löw, and T. Pfau, *Physical Review Letters* **130**, 023002 (2023).
- [17] P. Weckesser, F. Thielemann, D. Wiater, A. Wojciechowska, L. Karpa, K. Jachymski, M. Tomza, T. Walker, and T. Schaetz, *Nature* **600**, 429 (2021).
- [18] H. Hirzler, R. S. Lous, E. Trimby, J. Pérez-Ríos, A. Safavi-Naini, and R. Gerritsma, *Physical Review Letters* **128**, 103401 (2022).
- [19] O. Katz, M. Pinkas, N. Akerman, and R. Ozeri, *Nature Physics* **18**, 533 (2022).
- [20] T. Feldker, H. Fürst, H. Hirzler, N. V. Ewald, M. Mazzanti, D. Wiater, M. Tomza, and R. Gerritsma, *Nature Physics* **16**, 413 (2020).
- [21] M. Cetina, A. T. Grier, and V. Vuletić, *Physical Review Letters* **109**, 253201 (2012).
- [22] M. Pinkas, O. Katz, J. Wengrowicz, N. Akerman, and R. Ozeri, “Observation of trap-assisted formation of atom-ion bound states,” (2022).
- [23] H. Hirzler, E. Trimby, R. Gerritsma, A. Safavi-Naini, and J. Pérez-Ríos, *Physical Review Letters* **130**, 143003 (2023).
- [24] C. Schneider, M. Enderlein, T. Huber, and T. Schaetz, *Nature Photonics* **4**, 772 (2010).
- [25] T. Huber, A. Lambrecht, J. Schmidt, L. Karpa, and T. Schaetz, *Nature Communications* **5**, 5587 (2014).
- [26] J. Schmidt, A. Lambrecht, P. Weckesser, M. Debatin, L. Karpa, and T. Schaetz, *Physical Review X* **8**, 021028 (2018).
- [27] J. Schmidt, P. Weckesser, F. Thielemann, T. Schaetz, and L. Karpa, *Physical Review Letters* **124**, 053402 (2020).
- [28] T. F. Gloger, P. Kaufmann, D. Kaufmann, M. T. Baig, T. Collath, M. Johanning, and C. Wunderlich, *Physical Review A* **92**, 043421 (2015).
- [29] R. Grimm, M. Weidemüller, and Y. B. Ovchinnikov,

- in *Advances In Atomic, Molecular, and Optical Physics*, Vol. 42, edited by B. Bederson and H. Walther (Elsevier, 2000) pp. 95–170.
- [30] D. J. Berkeland, J. D. Miller, J. C. Bergquist, W. M. Itano, and D. J. Wineland, *Journal of Applied Physics* **83**, 5025 (1998).
- [31] M. Drewsen and A. Brøner, *Physical Review A* **62**, 045401 (2000).
- [32] See Supplemental Material at [URL] for details of the ion dynamics in the hybrid trap potential (Sec. I), details of ion eMM temperature with experiment imperfections (Sec.II), ion-atom Collision simulation (Sec. III), and the work down by RF field on the ion in hybrid trap (Sec. IV).
- [33] Z.-H. Qian, J.-M. Cui, X.-W. Luo, Y.-X. Zheng, Y.-F. Huang, M.-Z. Ai, R. He, C.-F. Li, and G.-C. Guo, *Physical Review Letters* **127**, 263603 (2021).
- [34] V. Blums, M. Piotrowski, M. I. Hussain, B. G. Norton, S. C. Connell, S. Gensemer, M. Lobino, and E. W. Streed, *Science Advances* **4**, eaao4453 (2018).
- [35] J. D. Wong-Campos, K. G. Johnson, B. Neyenhuis, J. Mizrahi, and C. Monroe, *Nature Photonics* **10**, 606 (2016).
- [36] R. He, J.-M. Cui, R.-R. Li, Z.-H. Qian, Y. Chen, M.-Z. Ai, Y.-F. Huang, C.-F. Li, and G.-C. Guo, *Review of Scientific Instruments* **92**, 073201 (2021).

# Supplemental Material: Cold hybrid electrical-optical ion trap

Jin-Ming Cui,<sup>1,2,3,\*</sup> Shi-Jia Sun,<sup>1,2</sup> Xi-Wang Luo,<sup>1,2,3</sup> Yun-Feng

Huang,<sup>1,2,3</sup> Chuan-Feng Li,<sup>1,2,3</sup> and Guang-Can Guo<sup>1,2,3</sup>

<sup>1</sup>*CAS Key Laboratory of Quantum Information,*

*University of Science and Technology of China, Hefei 230026, China*

<sup>2</sup>*CAS Center for Excellence in Quantum Information and Quantum Physics,*

*University of Science and Technology of China, Hefei 230026, China*

<sup>3</sup>*Hefei National Laboratory, University of Science*

*and Technology of China, Hefei 230088, China*

(Dated: June 21, 2023)

## ION DYNAMICS IN THE HYBRID TRAP POTENTIAL

The electrical potential of a classical Paul trap is

$$U_{\text{Paul}}(\mathbf{r}, t) = U_E(\mathbf{r}) + \tilde{U}_E(\mathbf{r}) \cos(\Omega t), \quad (\text{S1})$$

where  $U_E(\mathbf{r})$  and  $\tilde{U}_E(\mathbf{r})$  are the potentials generated by the DC and RF fields respectively. For a symmetric linear Paul trap with four rods or blades, the electrical potentials can be expressed as [1]

$$U_E(\mathbf{r}) = k_0 z^2 - \frac{1}{2} k_0 (x^2 + y^2), \quad (\text{S2})$$

$$\tilde{U}_E(\mathbf{r}) = k_1 (x^2 - y^2) + V_{RF}/2, \quad (\text{S3})$$

where  $k_0 = \kappa Q V_{DC}/Z_0^2$ ,  $k_1 = Q V_{RF}/2R^2$ , where  $\kappa$  is a geometric factor of the trap,  $Q$  is the charge of the ion,  $V_{DC}$  and  $V_{RF}$  are the DC and RF voltages applied on the trap,  $R$  is the perpendicular distance from the trap axis to the trap electrodes,  $Z_0$  is the distance from the trap center to the end-cap electrodes. The equations of motion for a single ion of mass  $m$  in the above potential are given by Mathieu equations

$$\ddot{u}_l + [a_{0,l} + 2q_{0,l} \cos(\Omega t)] \frac{\Omega^2}{4} u_l = 0, \quad (\text{S4})$$

where  $\mathbf{u} = u_x \hat{x} + u_y \hat{y} + u_z \hat{z}$  is the position of the ion and

$$a_{0,x} = a_{0,y} = -\frac{1}{2} a_z = \frac{4k_0}{m\Omega^2}, \quad (\text{S5})$$

$$q_{0,x} = -q_{0,y} = \frac{4k_1}{m\Omega^2}, \quad (\text{S6})$$

$$q_{0,z} = 0. \quad (\text{S7})$$

The potential generated by the hybrid trap is,

$$U(\mathbf{r}, t) = U_E(\mathbf{r}) + \tilde{U}_E(\mathbf{r}) \cos(\Omega t) + \sum_{i=1} U_{D,i}(\mathbf{r}) [1 + \eta_i \cos(\Omega t)], \quad (\text{S8})$$

$$= \Phi_0(\mathbf{r}) + \Phi_1(\mathbf{r}) \cos(\Omega t) \quad (\text{S9})$$

where  $U_{D,i}(\mathbf{r})$  is the potential of  $i$ 'th ODT,  $\eta_i$  is the modulation depth of the ODT,  $\Phi_0(\mathbf{r}) = U_E(\mathbf{r}) + \sum_i^N U_{D,i}(\mathbf{r})$  and  $\Phi_1(\mathbf{r}) = \tilde{U}_E(\mathbf{r}) + \sum_i^N \eta_i U_{D,i}(\mathbf{r})$  are the direct and alternating potentials respectively. If we use the two dipole trap scheme in the main text and use the



zero alternating trapping condition, the modulation parameters will be  $\eta_1 = -\eta_2 = 1$ . The potential of ODTs are [2]

$$U_D(\mathbf{r}) = \frac{\pi c^2 \Gamma}{2\omega_0^3} \left( \frac{2}{\Delta_2} + \frac{1}{\Delta_1} \right) I(\mathbf{r}), \quad (\text{S10})$$

where  $I(\mathbf{r})$  is the intensity of the specified ODT,  $\Gamma$  is the damping rate of  $P$  state,  $\Delta_2$  is the laser detuning from  $S_{1/2}$  to  $P_{3/2}$  transition,  $\Delta_1$  is the laser detuning from  $S_{1/2}$  to  $P_{1/2}$  transition, and  $\omega_0$  is the ODT laser frequency. The intensity profile of a focused astigmatic Gaussian beam along axis  $\hat{c}$  in coordinate  $(\hat{a}, \hat{b}, \hat{c})$  can be written as

$$I(\mathbf{r}) = I_0 \frac{w_{0a}}{w_a(c)} \frac{w_{0b}}{w_b(c)} \exp \left\{ -2 \left[ \frac{a^2}{w_a(c)^2} + \frac{b^2}{w_b(c)^2} \right] \right\}, \quad (\text{S11})$$

where  $w_{a/b}(c) = w_{0,a/b} \sqrt{1 + (c/z_{Ra/b})^2}$  are the beam waists for  $a$  and  $b$  axes, i. e. short and long axes respectively,  $z_{Ra/b} = \pi w_{0,a/b}^2 / \lambda$  are the Rayleigh ranges and  $\lambda$  is the ODT laser wavelength. Applying the scheme with two orthogonal astigmatic Gaussian beam spots at  $z = 0$  in the main text, the potentials are

$$\Phi_0(x, y, 0) = k_0 z^2 - \frac{1}{2} k_0 (x^2 + y^2) + U_0 \exp(-2x^2/w_a^2 - 2y^2/w_b^2) + U_0 \exp(-2x^2/w_b^2 - 2y^2/w_a^2),$$

$$\Phi_1(x, y, 0) = k_1 (x^2 - y^2) + U_0 \exp(-2x^2/w_a^2 - 2y^2/w_b^2) - U_0 \exp(-2x^2/w_b^2 - 2y^2/w_a^2),$$

where  $U_0 = \pi c^2 \Gamma (\Delta_2 + 2\Delta_1) I_0 / 2\omega_0^2 \Delta_2 \Delta_1$ . Expanding  $\Phi_1(x, y, 0)$  near the trap center ( $x = 0$ ,  $y = 0$ ) and setting it to zero, we can realize the zero alternating potential condition (ZATC),

$$U_0 = \frac{k_1 w_a^2 w_b^2}{2(w_a^2 - w_b^2)}. \quad (\text{S12})$$

To study three-dimensional dynamics of a single ion in the hybrid trap, we can perform numerical simulation by reserving the full form of the potentials. We take the equation along the  $x$  axis for example. From the equation of motion driven by forces

$$m\ddot{x} = -\frac{\partial U(\mathbf{r}, t)}{\partial x} = -\frac{\partial \Phi_0}{\partial x} - \frac{\partial \Phi_1}{\partial x} \cos(\Omega t), \quad (\text{S13})$$

we can get

$$\ddot{x} + [a_x(x, y, z) + 2q_x(x, y, z) \cos(\Omega t)] \frac{\Omega^2}{4} x = 0, \quad (\text{S14})$$

where

$$a_x(x, y, z) = \frac{4}{m\Omega^2} \frac{\partial \Phi_0}{x \partial x},$$

$$q_x(x, y, z) = \frac{2}{m\Omega^2} \frac{\partial \Phi_1}{x \partial x},$$

are Mathieu equation parameters that depend on the ion's position. The position dependent Mathieu equation parameters in three dimensions can be deduced as

$$\begin{aligned} a_x(x, y, z) &= \frac{4}{m\Omega^2} \left[ -k_0 - U_0 g(z) \left( f_1(x, y, z) \frac{4}{w_a^2(z)} + f_2(x, y, z) \frac{4}{w_b^2(z)} \right) \right], \\ a_y(x, y, z) &= \frac{4}{m\Omega^2} \left[ -k_0 - U_0 g(z) \left( f_1(x, y, z) \frac{4}{w_b^2(z)} + f_2(x, y, z) \frac{4}{w_a^2(z)} \right) \right], \\ a_z(x, y, z) &= \frac{4}{m\Omega^2} [2k_0 + U_0 g(z) (f_1 M_1 + f_2 M_2) + U_0 N(z) (f_1 + f_2)], \end{aligned} \quad (\text{S15})$$

and

$$\begin{aligned} q_x(x, y, z) &= \frac{2}{m\Omega^2} \left[ 2k_1 + U_0 g(z) \left( f_1(x, y, z) \frac{4}{w_a^2(z)} - f_2(x, y, z) \frac{4}{w_b^2(z)} \right) \right], \\ q_y(x, y, z) &= \frac{2}{m\Omega^2} \left[ -2k_1 + U_0 g(z) \left( f_1(x, y, z) \frac{4}{w_b^2(z)} - f_2(x, y, z) \frac{4}{w_a^2(z)} \right) \right], \\ q_z(x, y, z) &= \frac{2}{m\Omega^2} [U_0 g(z) (f_1 M_1 - f_2 M_2) + U_0 N(z) (f_1 - f_2)], \end{aligned} \quad (\text{S16})$$

where

$$\begin{aligned} f_1(x, y, z) &= \exp \left[ -2x^2/w_a^2(z) - 2y^2/w_b^2(z) \right] \\ f_2(x, y, z) &= \exp \left[ -2x^2/w_b^2(z) - 2y^2/w_a^2(z) \right] \\ g(z) &= \frac{1}{\sqrt{1 + (z/z_{Ra})^2} \sqrt{1 + (z/z_{Rb})^2}} \\ N(z) &= -g(z) \left( \frac{1}{z_{Ra}^2 + z^2} + \frac{1}{z_{Rb}^2 + z^2} \right) \\ M_1(x, y, z) &= \frac{4x^2}{w_{0,a}^2 z_{Ra}^2 \alpha_a^4(z)} + \frac{4y^2}{w_{0,b}^2 z_{Rb}^2 \alpha_b^4(z)} \\ M_2(x, y, z) &= \frac{4x^2}{w_{0,b}^2 z_{Rb}^2 \alpha_b^4(z)} + \frac{4y^2}{w_{0,a}^2 z_{Ra}^2 \alpha_a^4(z)} \end{aligned}$$

and  $w_{a/b}^2(z) = w_{0,a/b}^2 \alpha_{a/b}^2(z)$ ,  $\alpha_{a/b}(z) = \sqrt{1 + (z/z_{Ra/b})^2}$ ,  $z_{Ra/b} = \pi w_{0,a/b}^2 / \lambda$ .

In the presence of a stray electrical field  $\mathbf{E} = E_x \hat{x} + E_y \hat{y} + E_z \hat{z}$ , the equations of motion will be

$$\begin{aligned} \ddot{x} + [a_x(x, y, z) + 2q_x(x, y, z) \cos(\Omega t)] \frac{\Omega^2}{4} x &= \frac{Q \cdot E_x}{m}, \\ \ddot{y} + [a_y(x, y, z) + 2q_y(x, y, z) \cos(\Omega t)] \frac{\Omega^2}{4} y &= \frac{Q \cdot E_y}{m}, \\ \ddot{z} + [a_z(x, y, z) + 2q_z(x, y, z) \cos(\Omega t)] \frac{\Omega^2}{4} z &= \frac{Q \cdot E_z}{m}. \end{aligned}$$

## ION EMM TEMPERATURE WITH EXPERIMENT IMPERFECTIONS

### Micromotion temperature of a trapped ion

The Mathieu equation when DC field  $\vec{E}$  shifts the equilibrium position of the ion writes Berkeland *et al.* [1]

$$\ddot{u}_l + [a_l + 2q_l \cos(\Omega t)] \frac{\Omega^2}{4} u_l = \frac{Q \cdot E_l}{m},$$

and the solution is

$$u_l(t) = (u_{0,l} + u_{1,l} \cos(\omega_l t + \varphi_l)) \left( 1 + \frac{q_l}{2} \cos(\Omega t) \right),$$

where the equilibrium position

$$u_{0,l} \cong \frac{4Q \cdot E_l}{m\Omega^2(a_l + q_l^2/2)}.$$

The average kinetic energy due to motion along  $\hat{u}_l$  is

$$E_{k,l} = \frac{1}{4} m u_{1,l}^2 (\omega_l^2 + \frac{1}{8} q_l^2 \Omega^2) + \frac{m\Omega^2}{16} q_l^2 u_{0,l}^2,$$

where the second term represents the equivalent temperature for the kinetic energy due to excess micromotion along  $\hat{u}_l$ . So the temperature caused by excess micromotion in all directions reads

$$T_{\text{eMM}} = \sum_l \frac{E_{k,l}}{k_B} = \frac{m\Omega^2}{16k_B} \sum_l q_l^2 u_{0,l}^2, \quad (\text{S17})$$

and  $T_{\text{eMM}}$  represents the lowest attainable temperature caused by excess micromotion of an ion in the trap.

Now we consider the case that the Mathieu equation parameters are in a position-dependent form:  $a_l(\mathbf{u})$ ,  $q_l(\mathbf{u})$ . If the ion oscillates near  $\mathbf{u}_0$  in the hybrid trap under a stray electrical field  $\mathbf{E}$ , and it has been cooled to a low temperature  $|\mathbf{u} - \mathbf{u}_0| \ll w_a$ , then the Mathieu equation can be approximated as

$$\ddot{u}_l + [a_l(\mathbf{u}_0) + 2q_l(\mathbf{u}_0) \cos(\Omega t)] \frac{\Omega^2}{4} u_l = \frac{Q \cdot E_l}{m}, \quad (\text{S18})$$

where the equilibrium position  $\mathbf{u}_0$  can be numerically solved by iterating

$$u_{0,l}^{i+1} = \frac{4Q \cdot E_l}{m\Omega^2 [a_l(\mathbf{u}_0^i) + q_l^2(\mathbf{u}_0^i)/2]},$$

with an initial position  $\mathbf{u}_0^0 = (0, 0, 0)$ . Once the equilibrium position  $\mathbf{u}_0$  is solved, we can get the temperature caused by excess micromotion

$$T_{\text{eMM}} = \frac{m\Omega^2}{16k_B} \sum_l q_l^2(\mathbf{u}_0) u_{0,l}^2. \quad (\text{S19})$$

### Approximated ion's eMM temperature expression

Take Paul trap center as the origin of coordinate, supposing we use full modulation, and the misalignment between the Paul trap and the ODT is  $\delta x$ . We define  $\Delta x = x - \delta x$ , then we can approximate

$$\begin{aligned}
 a_x(x, 0, 0) &= \frac{4}{m\Omega^2} \left[ -k_0 - U_0 \left( e^{-2\Delta x^2/w_a^2} \frac{4}{w_a^2} + e^{-2\Delta x^2/w_b^2} \frac{4}{w_b^2} \right) \right] \\
 &\approx -\frac{4}{m\Omega^2} [k_0 + 2k_a + 2k_b - 4(k_a/w_a^2 + k_b/w_b^2) \Delta x^2] \\
 &= a - (x - \delta x)^2/x_a^2, \\
 q_x(x, 0, 0) &= \frac{2}{m\Omega^2} \left[ 2k_1 + U_0 \left( e^{-2\Delta x^2/w_a^2} \frac{4}{w_a^2} - e^{-2\Delta x^2/w_b^2} \frac{4}{w_b^2} \right) \right] \\
 &\approx \frac{4}{m\Omega^2} [k_1 + (k_a - k_b) + 2(k_b/w_b^2 - k_a/w_a^2) \Delta x^2] \\
 &= \Delta q + (x - \delta x)^2/x_b^2,
 \end{aligned} \tag{S20}$$

where  $k_{a,b} = 2U_0/w_{a,b}^2$ ,  $a = -4(k_0 + 2k_a + 2k_b)/m\Omega^2$ ,  $\Delta q = 4(k_1 + k_a - k_b)/m\Omega^2$ ,  $x_a^2 = -m\Omega^2/16(k_a/w_a^2 + k_b/w_b^2)$  and  $x_b^2 = m\Omega^2/8(k_b/w_b^2 - k_a/w_a^2)$ . The trap center will shift to an equilibrium position under a stray field  $E$

$$x_0 = \frac{4Q \cdot E}{m\Omega^2(a + \Delta q^2/2)} \approx \frac{4Q \cdot E}{m\Omega^2 a} = -\frac{Q \cdot E}{k_0 + 2k_a + 2k_b}.$$

Combined with Eq. S17, the approximated eMM temperature expression in this situation reads

$$\begin{aligned}
 T_{\text{eMM}} &\approx \frac{m\Omega^2}{16k_B} q_x^2(x_0, 0, 0) x_0^2 \\
 &\approx \frac{m\Omega^2}{16k_B} \left( \Delta q + \frac{(x_0 - \delta x)^2}{x_b^2} \right)^2 x_0^2,
 \end{aligned}$$

which clearly illustrates the roles that imperfections  $\Delta q$ ,  $\delta x$  play in restricting the lowest attainable temperature. In this expression, we approximate the iterated equilibrium position  $u_0$  to  $x_0$ , which represents the equilibrium position when no imperfections are presented. If we want the expression to be more precise, we could simply substitute  $x_0$  into the right side of the iteration formula in Eq. S19, and then let  $u_0$  equal to the first iteration solution  $x_1 = 4Q \cdot E / (m\Omega^2 [a_x(x_0, 0, 0) + q_x^2(x_0, 0, 0)/2])$ , which gives

$$T_{\text{eMM}} \approx \frac{m\Omega^2}{16k_B} \left( \Delta q + \frac{(x_1 - \delta x)^2}{x_b^2} \right)^2 x_1^2.$$

## ION-ATOM COLLISION 3D SIMULATION

In this section a numerical simulation method used for calculating the classical low-energy three-dimensional ion-atom collision trajectory is introduced. We simulated and compared two situations: the collision happens in a normal Paul trap and the hybrid trap we proposed, respectively. In the following content, we introduce how to calculate the collision process that happened in the hybrid trap, and the situation that happened in the Paul trap can be similarly and easily deduced.

An  $^{87}\text{Rb}$  atom of mass  $m_a$  approaches an  $^{172}\text{Yb}^+$  ion of mass  $m_i$  (initially resting in the center of the hybrid trap) from an arbitrary position (in the following content, we take the initial position as  $x = 100$  nm,  $y = 100$  nm,  $z = 100$  nm without loss of generality), by the attractive force between the two, the potential of which originates from the interaction between the ion and polarized atom and thus has the form  $-C_4/r^4$ , where  $C_4$  represent the polarizability of atom and the value of  $C_4$  is taken from Ref. [3]. For our selected  $^{87}\text{Rb}$ - $^{172}\text{Yb}^+$  pair,  $C_4 = 160E_h a_0^4$ , where  $E_h$  is the Hartree energy and  $a_0$  is the Bohr radius. At short ranges, we add a repulsive  $r^{-6}$  term to simulate a hard-core potential, where the hard-core collision distance is on the order of nm when the coefficient  $C_6$  is given as a fraction of  $C_4$ ,  $C_6 = (10a_0)^2 \times C_4$  in our simulation. Therefore, the total ion-atom potential reads

$$V(r) = -C_4/r^4 + C_6/r^6.$$

Since we intentionally select the magic wavelength  $\lambda = 422.3$  nm of the  $^{87}\text{Rb}$  atom as the ODT laser wavelength, the only potential experienced by the atom when approaching or moving away is the  $V(R)$  above. Thus, the equation of motion of the atom reads

$$m_a \frac{d^2 \mathbf{r}_a}{dt^2} = -\frac{4C_4}{(\mathbf{r}_a - \mathbf{r}_i)^6} (\mathbf{r}_a - \mathbf{r}_i) + \frac{6C_6}{(\mathbf{r}_a - \mathbf{r}_i)^8} (\mathbf{r}_a - \mathbf{r}_i), \quad (\text{S21})$$

where  $\mathbf{r}_a = (x_a, y_a, z_a)$  and  $\mathbf{r}_i = (x_i, y_i, z_i)$  are the 3D positions of atom and ion separately.

Combining Eq. S14 and the attractive force from the polarized atom, the equation of motion of the ion along the  $x$  direction is

$$m_i \frac{d^2 x_i}{dt^2} = -\frac{m_i \Omega^2}{4} [a_x(r_i) + 2q_x(r_i) \cos(\Omega t + \varphi)] x_i + \frac{4C_4}{(r_a - r_i)^6} (x_a - x_i), \quad (\text{S22})$$

and the equations of motion of the ion along the  $y$  and  $z$  direction can be written down similarly.

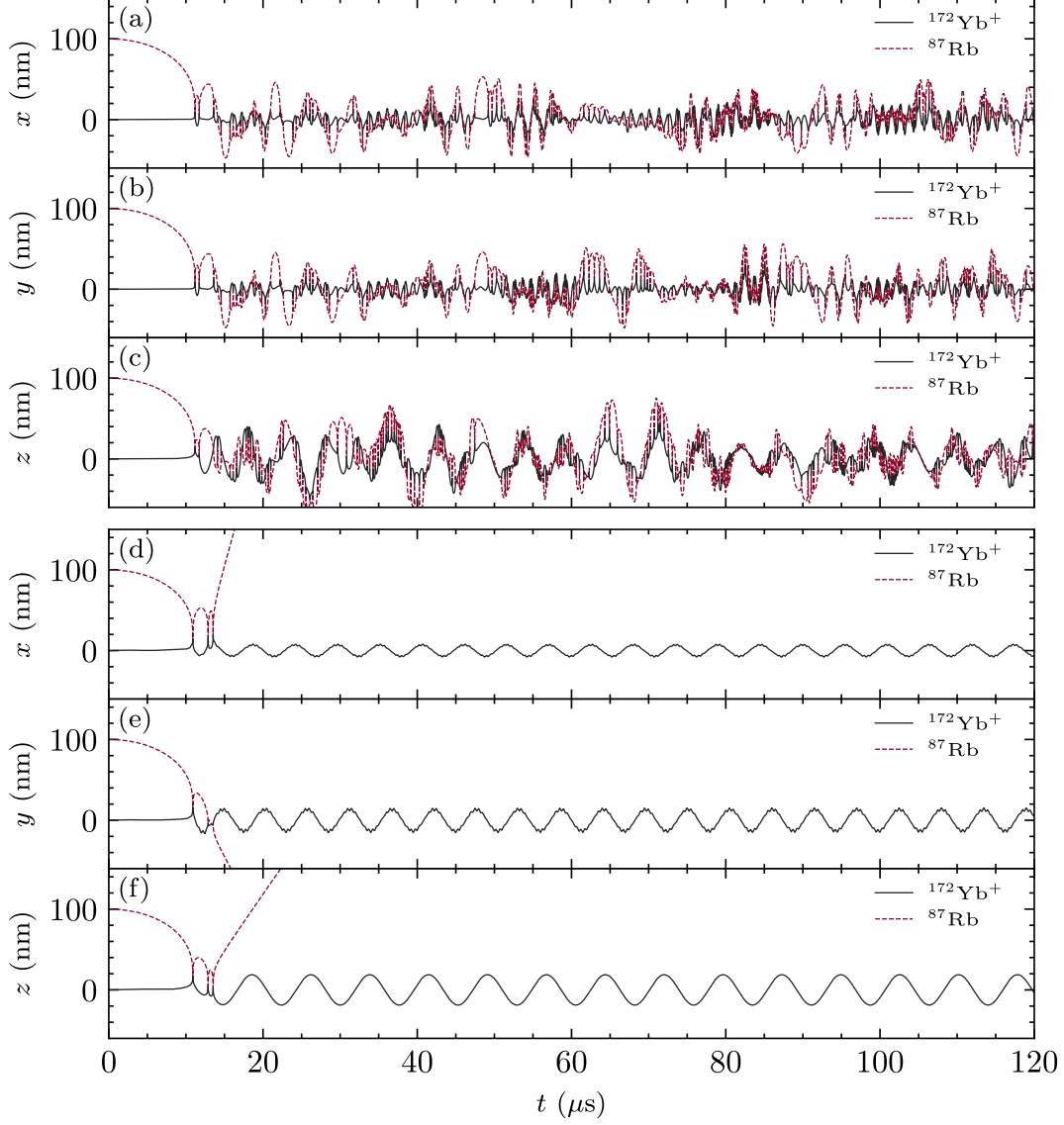


FIG. S1. Numerical 3D simulations of an ion-atom ( $^{87}\text{Rb}$  and  $^{172}\text{Yb}^+$ ) collision in a hybrid trap (a-c) and a Paul trap (d-f).

We use the explicit Runge-Kutta method of order eight to solve the equations of motion with Eq. S15, Eq. S16, Eq. S21 and Eq. S22. Fig. S1 shows a simulated collision trajectory of an atom-ion pair in  $x$ ,  $y$  and  $z$  directions respectively. The lifetime of the bound atom-ion pair produced in the hybrid trap is significantly prolonged due to the low RF heating near the hybrid trap center.

## WORK DONE BY RF FIELD ON THE ION

When an ion moves in a Paul trap without any disturbance, the RF field does zero work on the ion for an RF period. However, in a cold hybrid ion-atom system, the polarized atom will exert an attraction force on the ion (by attraction potential  $V(r) = -C_4/r^4$ ) and thus disturb the conserved cycle of energy transfer, and finally, the ion-atom system gains net energy from the RF field, which increases the temperature of the system. Here, we calculate the work done by the RF field on the ion when an atom approaches the ion and the collision happens. Suppose the collision point is at  $r_c$ , and the collision happens at  $t = 0$ . When the attraction force between the ion-atom pair dominates, the distance between the ion and atom follows  $r(t) = (18C_4/\mu)^{1/6}|t|^{1/3}$ , so the trajectory of the ion becomes  $r_i(t) = r_c - \mu r(t)/m_i$ , where  $\mu = m_i m_a / (m_i + m_a)$  is the reduced mass of the ion-atom pair. We can write down the work done by the RF field on the ion when the atom is close enough to perturb the motion of ion in the trap

$$W = \int_{-t_1}^{t_1} 2q(r_i) \cdot \frac{m_i \Omega^2}{4} r_i \cos(\Omega t + \phi) \dot{r}_i dt,$$

where integration range  $t = -t_1 \sim t_1$  is the time when the perturbation from the atom dominates, and we can take  $t_1 \approx 0.8$  for approximation[4]. By substituting Eq. S20 and the trajectory of the ion, we get the work done by the RF field during one collision

$$\begin{aligned} W &= W_1 + W_2, \\ W_1 &= \frac{1}{3} \mu \Omega^2 R^2 \sin \phi \cdot \Delta q \int_0^{\Omega t_1} (A - B\tau^{1/3}) \cdot \tau^{-2/3} \sin \tau \cdot d\tau, \\ W_2 &= \frac{1}{3} \mu \Omega^2 R^2 \sin \phi \cdot \frac{R^4}{r_0^2 x_b^2} \int_0^{\Omega t_1} (A - B\tau^{1/3})^3 \cdot \tau^{-2/3} \sin \tau \cdot d\tau, \end{aligned}$$

where  $A = r_c r_0 / R^2$ ,  $B = \mu r_0^2 / m_i R^2$ ,  $r_0 = \sqrt[6]{18C_4 / \mu \Omega^2}$ .  $W_1$  comes from the uncompensated alternating force  $\Delta q$  and  $W_2$  comes from the dependence of  $q$  on position. For the first collision, when the atom approaches the ion from infinity, the collision happens at  $r_{c,0} = 1.11(m_a/m_i)^{5/6} R \approx 20.8$  nm [4], and the numerical results give the max work heating  $W_1/k_B \approx -85.2$  nK,  $W_2/k_B \approx 27.8$  nK for  $\Delta q = -0.001$  at  $\sin \phi = 1$ . Here we intentionally choose  $\Delta q$  as negative because we want  $q(r)$  to be nearly 0 at the collision points, not at the origin.

After the first collision happens at  $r_{c,0}$ , the following collision position  $r_{c,i}$  for the  $i$ 'th collision is unpredictable. From Fig. S1(a,b) we see that the collisions most likely happen at

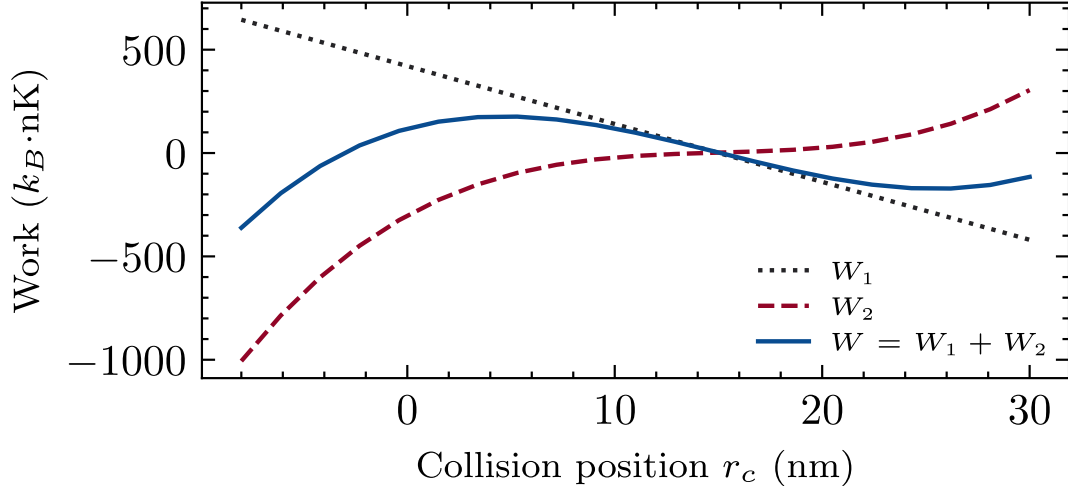


FIG. S2. Maximum work done by the RF field during one collision at  $\sin \phi = 1$ .

approximately  $0 \sim 20$  nm at micromotion directions ( $x$  and  $y$  axis). The Fig. S2 illustrates the relation of  $W = W_1 + W_2$  with  $r_c$  for  $\Delta q = -0.001$ , from which we could see that by compensating the  $\Delta q$  nearly zero, the work done by residual RF field during one collision is on the order of tens of  $\text{nK} \cdot k_B$ . Therefore, the relative energy between an ion-atom pair could easily run below the characteristic energy scale  $E_k$  after one or more collisions, making the formation of a bound state (like a molecular ion) possible.

J.-M. Cui and S.-J. Sun contributed equally to this work.

---

\* [jmcui@ustc.edu.cn](mailto:jmcui@ustc.edu.cn)

- [1] D. J. Berkeland, J. D. Miller, J. C. Bergquist, W. M. Itano, and D. J. Wineland, *Journal of Applied Physics* **83**, 5025 (1998).
- [2] R. Grimm, M. Weidemüller, and Y. B. Ovchinnikov, in *Advances In Atomic, Molecular, and Optical Physics*, Vol. 42, edited by B. Bederson and H. Walther (Elsevier, 2000) pp. 95–170.
- [3] M. Tomza, K. Jachymski, R. Gerritsma, A. Negretti, T. Calarco, Z. Idziaszek, and P. S. Julienne, *Reviews of Modern Physics* **91**, 035001 (2019).
- [4] M. Cetina, A. T. Grier, and V. Vuletić, *Physical Review Letters* **109**, 253201 (2012).